Appl. Math. Mech. -Engl. Ed., **44**(9), 1577–1596 (2023)

APPLIED MATHEMATICS AND MECHANICS (ENGLISH EDITION)

https://doi.org/10.1007/s10483-023-3031-8

On wave dispersion of rotating viscoelastic nanobeam based on general nonlocal elasticity in thermal environment*

A. RAHMANI[1], S. FAROUGHI[1,†], M. SARI[2]

1. Mechanical Engineering Faculty, Urmia University of Technology, Urmia 5716617165, Iran;
2. Mechanical and Maintenance Engineering Department, German Jordanian University, Amman 11180, Jordan

(Received May 2, 2023 / Revised Jul. 19, 2023)

Abstract The present research focuses on the analysis of wave propagation on a rotating viscoelastic nanobeam supported on the viscoelastic foundation which is subject to thermal gradient effects. A comprehensive and accurate model of a viscoelastic nanobeam is constructed by using a novel nonclassical mechanical model. Based on the general nonlocal theory (GNT), Kelvin-Voigt model, and Timoshenko beam theory, the motion equations for the nanobeam are obtained. Through the GNT, material hardening and softening behaviors are simultaneously taken into account during wave propagation. An analytical solution is utilized to generate the results for torsional (TO), longitudinal (LA), and transverse (TA) types of wave dispersion. Moreover, the effects of nonlocal parameters, Kelvin-Voigt damping, foundation damping, Winkler-Pasternak coefficients, rotating speed, and thermal gradient are illustrated and discussed in detail.

Key words temperature effect, general nonlocal theory (GNT), Kelvin-Voigt model, viscoelastic foundation, wave propagation, rotating viscoelastic nanobeam

Chinese Library Classification O343.6
2010 Mathematics Subject Classification 74J99, 97M50

1 Introduction

Viscoelastic nanobeams are structures that exhibit both viscous and elastic behaviors at the nanoscale. Their engineering background is primarily rooted in the fields of material science, nanotechnology, and mechanical engineering. These beams are typically composed of viscoelastic materials which possess time-dependent deformation characteristics. Viscoelastic nanobeams find applications in various areas due to their unique mechanical properties. Some applications are described as below.

Viscoelastic nanobeams are employed in microelectromechanical system (MEMS) and nanoelectromechanical system (NEMS) devices. These devices often require flexible and resilient components, and viscoelastic nanobeams provide the desired properties for sensing, actuation, and energy harvesting applications[1–3]. Viscoelastic nanobeams can be used as platforms for

* Citation: RAHMANI, A., FAROUGHI, S., and SARI, M. On wave dispersion of rotating viscoelastic nanobeam based on general nonlocal elasticity in thermal environment. *Applied Mathematics and Mechanics* (*English Edition*), **44**(9), 1577–1596 (2023) https://doi.org/10.1007/s10483-023-3031-8

† Corresponding author, E-mail: sh.farughi@uut.ac.ir

drug delivery systems. By incorporating drug-loaded nanoparticles into nanobeam structures, controlled release of drugs can be achieved through viscoelastic deformations of beams in response to external stimuli, such as temperature or pH changes[4–6]. In biomedical engineering, viscoelastic nanobeams find applications in tissue engineering, regenerative medicine, and biosensing. They can be used as scaffolds for cell growth and tissue regeneration, as well as in the development of biosensors for detecting specific biomarkers[7–9]. Viscoelastic nanobeams can be utilized for energy harvesting from ambient vibration. Their viscoelastic behavior allows them to efficiently convert mechanical vibration into electrical energy, which can be harnessed for powering small electronic devices or sensors[10–12].

When supported on viscoelastic foundations, viscoelastic nanobeams can exhibit enhanced mechanical properties and offer additional applications. By placing viscoelastic nanobeams on viscoelastic foundations, it is possible to create vibration isolation systems. These systems effectively attenuate vibrations transmitted through the nanobeams, making them useful in reducing the impact of external vibrations on sensitive equipments or structures[13–14]. Viscoelastic nanobeams supported on viscoelastic foundations can act as shock absorbers. When the beams and foundations are subject to sudden impacts or mechanical shocks, their viscoelastic nature allows them to dissipate energy and protect the surrounding structures or components[15–16]. When viscoelastic nanobeams are supported on viscoelastic substrates, they can be used as flexible interconnects or stretchable electrodes in electronic devices. The viscoelastic foundation enables mechanical flexibility and robustness, allowing nanobeams to withstand bending, stretching, or other deformations without losing functionality[17–18].

Overall, viscoelastic nanobeams offer a wide range of applications in diverse fields, including MEMS/NEMS, drug delivery, biomedical engineering, energy harvesting, vibration isolation, shock absorption, and flexible electronics. These applications leverage the unique properties of viscoelastic materials and the nanoscale engineering of beams to achieve desired functionalities. Hence, small viscoelastic structures such as viscoelastic nanobeams have attracted great attention due to their exceptional properties and characteristics.

It is known that experimental and statistical approaches can demonstrate the impacts of small-scale effects on the behavior of nanostructures. However, these methods are costly, time-consuming, and restricted by the capabilities of technical facilities. On the other hand, as the continuum theories are scale-free, they are incapable of capturing the influence of small-scale parameters on the performance of nanostructures[19–21]. Different theories that consider small-scale effects have been proposed, such as the nonlocal theory[22–24], the strain gradient theory[25–26], the modified coupled stress theory[27–28], and the nonlocal strain gradient theory[29–31]. The nonlocal strain gradient theory is an advanced theoretical framework that incorporates both strain gradients and nonlocal effects to better describe the mechanical behavior of materials at small scales. This theory takes into account the influence of microstructural features and interactions, such as dislocations and grain boundaries, on the overall deformation response of materials. By considering strain gradients, which capture the variations in strain within materials, and nonlocal effects, accounting for the influence of neighboring regions, the nonlocal strain gradient theory provides a more comprehensive understanding of material behavior at the microscale and nanoscale.

Nanostructures with the ability to rotate and spin, such as nanogears, nanoturbines, and nanobearings, have garnered significant interest among nanotechnology researchers. The reliable design and formulation of these structures necessitate a thorough investigation of vibration and wave dispersion of nanobeams. For instance, in a study by Khaniki[32], the vibration of rotating nanobeams was examined using Eringen's two-phase local/nonlocal theory. The natural frequencies were obtained through the utilization of a modified generalized differential quadrature method. The study demonstrated that the dynamical behavior of the rotating nanobeams is significantly influenced by the scale parameter, rotating speed, and hub radius. Fang et al.[33] employed the nonlocal elasticity theory to investigate the natural vibrations of rotating

nanobeams with functionally graded (FG) material properties varying along their thickness. The displacement field incorporated an axial shortening term, and the model was derived using Hamilton's principle. Galerkin's approach was then utilized to solve the resulting equations. The study revealed that the natural frequencies of the rotating nanobeams are significantly influenced by the nonlocal parameter, slenderness ratio, angular velocity, and FG index. Additionally, Ebrahimi and Haghi[34] examined the wave dispersion behavior of a rotating FG Euler-Bernoulli beam model. The mathematical model was formulated using the nonlocal strain gradient theory and Hamilton's principle. Closed-form solutions were presented, demonstrating the substantial impact of the angular velocity, temperature change, FG index, nonlocal parameter, and length scale parameter on the structural behavior. In another investigation, Ebrahimi and Dabbagh[35] applied the nonlocal strain gradient theory to analyze the wave dispersion characteristics of a rotating FG nanobeam subject to magnetic and electric fields. The material properties were assumed to vary through the thickness according to a power law relation. The analysis accounted for shear deformation, and the governing equations of motion were derived using Hamilton's principle. Analytical solutions were obtained, revealing the significant influences of shear deformation, angular velocity, nonlocal parameter, FG index, wave number, and magneto-electric potentials on the wave propagation of rotating FG nanobeams. Furthermore, Rahmani et al.[36] investigated the wave propagation behavior of rotating nanobeams in a thermal environment supported by a Winkler-Pasternak layer. The governing equations of motion were derived using Reddy's beam theory, nonlocal elasticity theory, modified couple stress theory, and Hamilton's principle. Analytical solutions were employed, demonstrating that the angular velocity, FG index, wave number, and nonlocal parameter have considerable impacts on the wave propagation behavior of rotating FG nanobeams. Ebrahimi et al.[37] developed an analytical solution for the wave dispersion characteristics of a rotating FG Euler-Bernoulli nanobeam. The governing equations of motion were obtained using Hamilton's principle and Eringen's nonlocal elasticity theory. Closed-form solutions were assumed, and it was illustrated that the angular velocity, FG index, wave number, and nonlocal parameter significantly affect the wave propagation behavior of rotating FG nanobeams.

When dealing with materials exhibiting distinct axial and transverse (TA) characteristics, Eringen's nonlocal theory (ENT) presents certain drawbacks and limitations. Recognizing this, Shaat[38] introduced the general elasticity theory as an alternative approach for modeling particle mechanics and material dispersion relations. Multiple attenuation functions were explored to ascertain the material coefficients and length scales.

Faroughi et al.[39] proposed a wave dispersion analysis for two-dimensional (2D) FG nanobeams. They employed the general nonlocal theory (GNT), Reddy's beam theory, and Hamilton's principle to formulate a model for porous rotating beams. The study revealed that the wave dispersion behavior of 2D rotating FG nanobeams is influenced by the FG indexes, porosity, nonlocal parameter, and rotating velocity. Rahmani et al.[40] utilized the GNT to investigate the vibrations of bi-directional rotating porous FG nanobeams. The governing equations of motion were derived using Reddy's beam theory and Hamilton's principle. The differential quadrature method was used to determine the natural frequencies of the nanobeams. The study discussed the effects of porosity, length-to-thickness ratio, power law indexes, and angular velocity on the free vibration. In another study, Faroughi and Shaat[41] examined the influence of Poisson's ratio on the bending and vibration behaviors of auxetic and non-auxetic nanobeams. The GNT was introduced to model the nonlocal effects. The findings emphasized the crucial role of Poisson's ratio in determining the characteristics of nanobeams. Li et al.[42] conducted an investigation into the vibrational behavior of rotating FG piezoelectric nanobeams. They utilized the Timoshenko beam model and the nonlocal elasticity theory to formulate the governing equations. The numerical results were obtained using the differential quadrature method. Wang et al.[43] performed a vibration analysis of rotating axisymmetric circular nanoplates. They employed the Mindlin plate theory, nonlocal strain gradient theory,

and differential quadrature method to derive the model and obtain the results.

After reviewing the existing literature, it is apparent that no studies have investigated the wave propagation of a viscoelastic nanobeam using the general nonlocal elasticity theory. Therefore, the objective of this research is to address this gap in the literature. Specifically, this study focuses on the analysis of wave propagation in a rotating viscoelastic nanobeam supported on a viscoelastic foundation and subject to thermal gradient effects. The mathematical model is established, and results are obtained by employing the GNT, Kelvin-Voigt model, Timoshenko beam theory, and an analytic method. The remainder of this study is organized as follows. Section 2 formulates the problem and utilizes Hamilton's principle to establish the governing equations of motion for a rotating Timoshenko nanobeam resting on a viscoelastic layer and subject to thermal loads. In Section 3, the GNT is introduced, along with two constant nonlocal moduli as functions of the lattice constant. Section 4 applies the Kelvin-Voigt model to illustrate the viscoelastic properties. Section 5 assumes a closed-form solution and estimates the results using an analytic method. The model is validated, and the results are presented and discussed in Section 6. Finally, Section 7 provides concluding remarks.

2 Formulation

Figure 1 shows a Kelvin-Voigt rotating nanobeam resting on a viscoelastic foundation. The geometric characteristics of the nanobeam with rectangular cross sections are L, b, and h for length, width, and thickness, respectively. Based on the Timoshenko beam model, the displacement fields are considered as

$$u_1(x,t) = u(x,t) - z\varphi(x,t), \quad u_2(x,t) = 0, \quad u_3(x,t) = w(x,t), \tag{1}$$

in which $\boldsymbol{u}\,(=(u_1,u_2,u_3))$ is the displacement in (x,y,z) directions. Also, u and w are longitudinal (LA) and TA displacements, respectively, and φ denotes the rotation of the cross section.

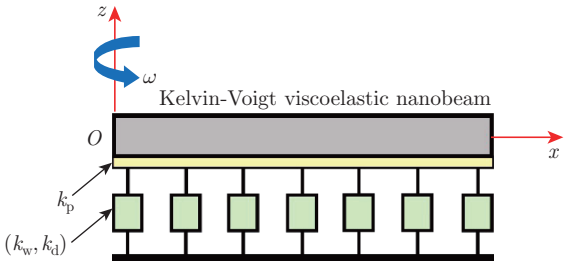

Fig. 1 Kelvin-Voigt rotating nanobeam (color online)

Therefore, the strains can be expressed as

$$\begin{cases} \varepsilon_{xx} = \dfrac{\partial u_1}{\partial x} = \dfrac{\partial u}{\partial x} - z\dfrac{\partial \varphi}{\partial x}, \\ 2\varepsilon_{xz} = \gamma_{xz} = \dfrac{\partial u_1}{\partial z} + \dfrac{\partial u_3}{\partial x} = \dfrac{\partial w}{\partial x} - \varphi. \end{cases} \tag{2}$$

Accordingly, the strain energy density Π_{s} can be expressed as follows:

$$\Pi_{\mathrm{s}} = \int_0^L \int_A (\sigma_{xx}\varepsilon_{xx} + \sigma_{xz}\gamma_{xz})\mathrm{d}A\mathrm{d}x = \int_0^L \Big(N_{xx}\frac{\partial u}{\partial x} - M_{xx}\frac{\partial \varphi}{\partial x} + N_{xy}\Big(\frac{\partial w}{\partial x} - \varphi\Big)\Big)\mathrm{d}x, \tag{3}$$

where

$$N_{xx} = \int_A \sigma_{xx} \mathrm{d}A, \quad M_{xx} = \int_A z\sigma_{xx} \mathrm{d}A, \quad N_{xy} = \int_A \sigma_{xy} \mathrm{d}A. \tag{4}$$

Also, the kinetic energy Π_{k} and the work of external forces Π_{w} are defined as

$$\begin{aligned} \Pi_{\mathrm{k}} &= \frac{1}{2}\rho \int_0^L \int_A \Big(\Big(\frac{\partial u_1}{\partial t}\Big)^2 + \Big(\frac{\partial u_2}{\partial t}\Big)^2 + \Big(\frac{\partial u_3}{\partial t}\Big)^2 \Big) \mathrm{d}A \mathrm{d}x \\ &= \frac{1}{2} \int_0^L \Big(m_0 \Big(\frac{\partial u}{\partial t}\Big)^2 - 2m_1 \Big(\frac{\partial u}{\partial t}\Big)\Big(\frac{\partial \varphi}{\partial t}\Big) + m_2 \Big(\frac{\partial \varphi}{\partial t}\Big)^2 + m_0 \Big(\frac{\partial w}{\partial t}\Big)^2 \Big) \mathrm{d}x, \end{aligned} \tag{5}$$

$$\Pi_{\mathrm{w}} = \int_0^L \Big(-\frac{\partial}{\partial x}\Big(N_{\mathrm{T}} \frac{\partial w}{\partial x}\Big) + q - k_{\mathrm{w}} w - k_{\mathrm{d}} \frac{\partial w}{\partial t} + k_{\mathrm{p}} \frac{\partial^2 w}{\partial x^2} + \frac{\partial}{\partial x}\Big(T(x) \frac{\partial w}{\partial x}\Big) + f \Big) \mathrm{d}x, \tag{6}$$

in which N_{T} ($= \int_A (E\alpha \Delta T) \mathrm{d}A$) is the thermal force applied due to thermal gradients. k_{w}, k_{d}, and k_{p} are the coefficients indicating the Winkler, damping, and Pasternak factors associated with the foundation, respectively. q and f are external forces acting in the TA and LA directions, respectively. When the nanobeam rotates, the axial force caused by centrifugal stiffening $T(x)$ is represented as

$$T(x) = b \int_x^L \int_{-h/2}^{h/2} \rho \omega_{\mathrm{b}}^2 x \mathrm{d}z \mathrm{d}x, \tag{7}$$

where ω_{b} is observed as the rotating speed of the nanobeam.

It is important to pay attention to the fact that the effects of temperature gradients at the nanoscale can deviate from classical macro-scale behavior due to several reasons, such as size effects, phonon transport, surface effects, and quantum effects. Nevertheless, the concept of thermal loads can still be applicable in small-size structures, and many recent research studies equate the effect of temperature gradients to thermal loads in small-scale structures[36,44–46]. However, this study ignores the effects of phonon transport, surface effects, and quantum effects.

Hence, in order to derive the mathematical model, Hamilton's principle can be applied as

$$\delta \Pi = \delta \int_{t_1}^{t_2} (\Pi_{\mathrm{s}} - \Pi_{\mathrm{k}} - \Pi_{\mathrm{w}}) \mathrm{d}t = 0. \tag{8}$$

Thus, the first variations of Π_{s}, Π_{k}, and Π_{w} give

$$\delta \Pi_{\mathrm{s}} = \int_0^L \Big(-\frac{\partial N_{xx}}{\partial x} \delta u + \Big(\frac{\partial M_{xx}}{\partial x} - N_{xy}\Big) \delta \varphi - \frac{\partial N_{xy}}{\partial x} \delta w \Big) \mathrm{d}x, \tag{9}$$

$$\delta \Pi_{\mathrm{k}} = -\int_0^L \Big(\Big(m_0 \frac{\partial^2 u}{\partial t^2} - m_1 \frac{\partial^2 \varphi}{\partial t^2} \Big) \delta u + \Big(m_2 \frac{\partial^2 \varphi}{\partial t^2} - m_1 \frac{\partial^2 u}{\partial t^2} \Big) \delta \varphi + \Big(m_0 \frac{\partial^2 w}{\partial t^2} \Big) \delta \varphi \Big) \mathrm{d}x, \tag{10}$$

$$\delta \Pi_{\mathrm{w}} = -\int_0^L \Big(\Big(-\frac{\partial}{\partial x}\Big(N_{\mathrm{T}} \frac{\partial w}{\partial x}\Big) + q - k_{\mathrm{w}} w - k_{\mathrm{d}} \frac{\partial w}{\partial t} + k_{\mathrm{p}} \frac{\partial^2 w}{\partial x^2} + \frac{\partial}{\partial x}\Big(T(x) \frac{\partial w}{\partial x}\Big) \Big) \delta w + f \delta u \Big) \mathrm{d}x. \tag{11}$$

Equations (9)–(11) can be substituted into Eq. (8) to derive the equations of motion as follows:

$$\delta u : -\frac{\partial N_{xx}}{\partial x} + f + m_0 \frac{\partial^2 u}{\partial t^2} = 0, \tag{12a}$$

$$\delta \varphi : \frac{\partial M_{xx}}{\partial x} - N_{xy} + m_2 \frac{\partial^2 \varphi}{\partial t^2} = 0, \tag{12b}$$

$$\delta w : -\frac{\partial N_{xy}}{\partial x} - \frac{\partial}{\partial x}\Big(N_{\mathrm{T}} \frac{\partial w}{\partial x}\Big) + q - k_{\mathrm{w}} w - k_{\mathrm{d}} \frac{\partial w}{\partial t} + k_{\mathrm{p}} \frac{\partial^2 w}{\partial x^2} + \frac{\partial}{\partial x}\Big(T(x) \frac{\partial w}{\partial x}\Big) + m_0 \frac{\partial^2 w}{\partial t^2} = 0. \tag{12c}$$

3 GNT

In the nonlocal fields, Shaat and Abdelkefi[47] introduced a novel nonlocal theory known as the GNT. Their research is aimed to advance ENT and provide fresh insights into its limitations. The authors demonstrated that the conventional nonlocal theory (i.e., the ENT) fails to simultaneously account for both LA and TA (shear) acoustic dispersions in materials. To overcome this limitation, they developed the GNT, which can accurately describe both hardening and softening behaviors. Consequently, the GNT utilized in their study is considered as the most comprehensive, suitable, and accurate theory for investigating elastic wave dispersion in materials.

Unlike the conventional nonlocal theory, the GNT employs two distinct nonlocal coefficients. With the GNT, the nonlocal stress fields can be expressed as follows[38,47]:

$$\sigma_{ji}(\boldsymbol{x}) = \int_V (\lambda\beta_1(|\boldsymbol{x}' - \boldsymbol{x}|)\varepsilon_{rr}(\boldsymbol{x}')\delta_{ij} + 2\mu\beta_2(|\boldsymbol{x}' - \boldsymbol{x}|)\varepsilon_{ij}(\boldsymbol{x}'))\mathrm{d}V', \tag{13}$$

in which σ_{ji} specifies the nonlocal stress field based on the two constant nonlocal coefficients $\beta_1(|\boldsymbol{x}' - \boldsymbol{x}|)$ and $\beta_2(|\boldsymbol{x}' - \boldsymbol{x}|)$. λ and μ are Lame's constants. Also, δ and ε_{ij} $\big(= \frac{1}{2}(u_{i,j} + u_{j,i})\big)$ denote the Dirac-delta function and the nonlocal strain field, respectively.

According to the GNT, the differential equation is indicated as[47]

$$(1 - \epsilon_1\nabla^2)(1 - \epsilon_2\nabla^2)\sigma_{(ji)}(\boldsymbol{x}) = \lambda(1 - \epsilon_2\nabla^2)\varepsilon_{rr}(\boldsymbol{x})\delta_{ij} + 2\mu(1 - \epsilon_1\nabla^2)\varepsilon_{ij}(\boldsymbol{x}), \tag{14}$$

where ϵ_1 and ϵ_2 are two constant nonlocal moduli which are described as functions of the lattice constant a, and $\nabla^2 = \frac{\partial^2}{\partial x^2}$ is the Laplacian gradient operator.

Based on the GNT, Eq. (14) can be rewritten as

$$(1 - \epsilon_1\nabla^2)(1 - \epsilon_2\nabla^2)\sigma_{xx} = \lambda(1 - \epsilon_2\nabla^2)\varepsilon_{xx} + 2\mu(1 - \epsilon_1\nabla^2)\varepsilon_{xx}, \tag{15a}$$

$$(1 - \epsilon_1\nabla^2)(1 - \epsilon_2\nabla^2)\sigma_{xy} = 2\mu(1 - \epsilon_1\nabla^2)\varepsilon_{xy}. \tag{15b}$$

Substituting Eq. (2) into Eq. (15) and paying attention to Eq. (4) give

$$(1 - \epsilon_1\nabla^2)(1 - \epsilon_2\nabla^2)N_{xx} = (1 - \epsilon_2\nabla^2)\Big(A_0\frac{\partial u}{\partial x} - A_1\frac{\partial \varphi}{\partial x}\Big) + 2(1 - \epsilon_1\nabla^2)\Big(B_0\frac{\partial u}{\partial x} - B_1\frac{\partial \varphi}{\partial x}\Big), \tag{16a}$$

$$(1 - \epsilon_1\nabla^2)(1 - \epsilon_2\nabla^2)M_{xx} = (1 - \epsilon_2\nabla^2)\Big(A_1\frac{\partial u}{\partial x} - A_2\frac{\partial \varphi}{\partial x}\Big) + 2(1 - \epsilon_1\nabla^2)\Big(B_1\frac{\partial u}{\partial x} - B_2\frac{\partial \varphi}{\partial x}\Big), \tag{16b}$$

$$(1 - \epsilon_1\nabla^2)(1 - \epsilon_2\nabla^2)N_{xy} = 2B_0(1 - \epsilon_1\nabla^2)\Big(\frac{\partial w}{\partial x} - \varphi\Big), \tag{16c}$$

where

$$(A_0, A_1, A_2) = \int_A \lambda(1, z, z^2)\mathrm{d}A, \tag{17a}$$

$$(B_0, B_1, B_2) = \kappa_{\mathrm{s}}\int_A \mu(1, z, z^2)\mathrm{d}A, \tag{17b}$$

in which κ_{s} is the shear correction factor in the Timoshenko beam model, and it is equal to 5/6 for square cross section.

Applying the GNT into Eq. (12) and considering Eq. (16) lead to the governing equations of motion for the rotating nanobeam resting on the viscoelastic foundation in terms of displacements as

$$\begin{aligned}\delta u\colon\ & (A_0 + 2B_0)\frac{\partial^2 u}{\partial x^2} - (\epsilon_2 A_0 + 2\epsilon_1 B_0)\frac{\partial^4 u}{\partial x^4} - (A_1 + 2B_1)\frac{\partial^2 \varphi}{\partial x^2} + (\epsilon_2 A_1 + 2\epsilon_1 B_1)\frac{\partial^4 \varphi}{\partial x^4} \\ & = m_0\Big(\frac{\partial^2 u}{\partial t^2} - (\epsilon_1 + \epsilon_2)\frac{\partial^4 u}{\partial x^2 \partial t^2} + \epsilon_1\epsilon_2\frac{\partial^6 u}{\partial x^4 \partial t^2}\Big),\end{aligned} \tag{18a}$$

$$\begin{aligned}\delta\varphi\colon\ & (A_1+2B_1)\frac{\partial^2 u}{\partial x^2}-(\epsilon_2A_1+2\epsilon_1B_1)\frac{\partial^4 u}{\partial x^4}+B_0\varphi-(A_2+2B_2+\epsilon_1B_0)\frac{\partial^2\varphi}{\partial x^2}\\ &+(\epsilon_2A_2+2\epsilon_1B_2)\frac{\partial^4\varphi}{\partial x^4}-B_0\frac{\partial w}{\partial x}+\epsilon_1B_0\frac{\partial^3 w}{\partial x^3}\\ &=-m_2\Big(\frac{\partial^2\varphi}{\partial t^2}-(\epsilon_1+\epsilon_2)\frac{\partial^4\varphi}{\partial x^2\partial t^2}+\epsilon_1\epsilon_2\frac{\partial^6\varphi}{\partial x^4\partial t^2}\Big),\end{aligned}\tag{18b}$$

$$\begin{aligned}\delta w\colon\ & B_0\frac{\partial\varphi}{\partial x}-\epsilon_1B_0\frac{\partial^3\varphi}{\partial x^3}+\epsilon_1\epsilon_2(k_{\mathrm{p}}-N_{\mathrm{T}}+T(x))\frac{\partial^6 w}{\partial x^6}+\epsilon_1\epsilon_2\Big(\frac{\partial T(x)}{\partial x}-\frac{\partial N_{\mathrm{T}}}{\partial x}\Big)\frac{\partial^5 w}{\partial x^5}\\ &+(\epsilon_1B_0+(\epsilon_1+\epsilon_2)(N_{\mathrm{T}}-T(x)-k_{\mathrm{p}})-\epsilon_1\epsilon_2k_{\mathrm{w}})\frac{\partial^4 w}{\partial x^4}+(\epsilon_1+\epsilon_2)\Big(\frac{\partial N_{\mathrm{T}}}{\partial x}-\frac{\partial T(x)}{\partial x}\Big)\frac{\partial^3 w}{\partial x^3}\\ &+\Big(T(x)-N_{\mathrm{T}}-B_0+k_{\mathrm{p}}+(\epsilon_1+\epsilon_2)\Big(\frac{\partial^2 N_{\mathrm{T}}}{\partial x^2}-\frac{\partial^2 T(x)}{\partial x^2}+k_{\mathrm{w}}\Big)\\ &-\epsilon_1\epsilon_2\Big(\frac{\partial^4 N_{\mathrm{T}}}{\partial x^4}-\frac{\partial^4 T(x)}{\partial x^4}\Big)\Big)\frac{\partial^2 w}{\partial x^2}+\Big(\frac{\partial T(x)}{\partial x}-\frac{\partial N_{\mathrm{T}}}{\partial x}+(\epsilon_1+\epsilon_2)\Big(\frac{\partial^3 N_{\mathrm{T}}}{\partial x^3}-\frac{\partial^3 T(x)}{\partial x^3}\Big)\Big)\frac{\partial w}{\partial x}\\ &-k_{\mathrm{w}}w-k_{\mathrm{d}}\Big(\frac{\partial w}{\partial t}-(\epsilon_1+\epsilon_2)\frac{\partial^3 w}{\partial x^2\partial t}+\epsilon_1\epsilon_2\frac{\partial^5 w}{\partial x^4\partial t}\Big)\\ &=-m_0\Big(\frac{\partial^2 w}{\partial t^2}-(\epsilon_1+\epsilon_2)\frac{\partial^4 w}{\partial x^2\partial t^2}+\epsilon_1\epsilon_2\frac{\partial^6 w}{\partial x^4\partial t^2}\Big).\end{aligned}\tag{18c}$$

It is noted that, for $\epsilon_1=\epsilon_2$, the GNT is reduced to the conventional ENT which was extensively employed in the previous studies.

4 Kelvin-Voigt model for nanobeam

The Kelvin-Voigt viscoelastic model states that the mechanical properties are dependent on the variation in time. Therefore, Lame's constants of materials are, respectively, defined as[48]

$$\lambda_{\mathrm{viscoelastic}}=\lambda\Big(1+C_{\mathrm{d}}\frac{\partial}{\partial t}\Big),\tag{19a}$$

$$\mu_{\mathrm{viscoelastic}}=\mu\Big(1+C_{\mathrm{d}}\frac{\partial}{\partial t}\Big),\tag{19b}$$

in which C_{d} is the damping parameter of the structure, and $\frac{\partial}{\partial t}$ is the derivative with respect to time.

Based on the Kevin-Voigt model and elasticity theory, the constitutive equation can be formulated as follows:

$$\sigma_{ij}(\boldsymbol{x})=\Big(1+C_{\mathrm{d}}\frac{\partial}{\partial t}\Big)(\lambda\varepsilon_{rr}(\boldsymbol{x})\delta_{ij}+2\mu\varepsilon_{ij}(\boldsymbol{x})).\tag{20}$$

On the basis of the GNT and Kelvin-Voigt viscoelastic models and substituting Eq. (20) into Eq. (3) and considering Eq. (16), the governing equations of motion for a rotating nanobeam on a viscoelastic foundation can be established as follows:

$$\delta u\colon\ \Big(1+C_{\mathrm{d}}\frac{\partial}{\partial t}\Big)\Delta_u=m_0\Big(\frac{\partial^2 u}{\partial t^2}-(\epsilon_1+\epsilon_2)\frac{\partial^4 u}{\partial x^2\partial t^2}+\epsilon_1\epsilon_2\frac{\partial^6 u}{\partial x^4\partial t^2}\Big),\tag{21a}$$

$$\delta\varphi\colon\ \Big(1+C_{\mathrm{d}}\frac{\partial}{\partial t}\Big)\Delta_\varphi=-m_2\Big(\frac{\partial^2\varphi}{\partial t^2}-(\epsilon_1+\epsilon_2)\frac{\partial^4\varphi}{\partial x^2\partial t^2}+\epsilon_1\epsilon_2\frac{\partial^6\varphi}{\partial x^4\partial t^2}\Big),\tag{21b}$$

$$\delta w\colon\ \Big(1+C_{\mathrm{d}}\frac{\partial}{\partial t}\Big)\Delta_w+\epsilon_1\epsilon_2(k_{\mathrm{p}}-N_{\mathrm{T}}+T(x))\frac{\partial^6 w}{\partial x^6}+\epsilon_1\epsilon_2\Big(\frac{\partial T(x)}{\partial x}-\frac{\partial N_{\mathrm{T}}}{\partial x}\Big)\frac{\partial^5 w}{\partial x^5}$$

$$
\begin{aligned}
&+((\epsilon_1+\epsilon_2)(N_{\mathrm{T}}-T(x)-k_{\mathrm{p}})-\epsilon_1\epsilon_2 k_{\mathrm{w}})\frac{\partial^4 w}{\partial x^4}+(\epsilon_1+\epsilon_2)\Big(\frac{\partial N_{\mathrm{T}}}{\partial x}-\frac{\partial T(x)}{\partial x}\Big)\frac{\partial^3 w}{\partial x^3}\\
&+(T(x)-N_{\mathrm{T}}+k_{\mathrm{p}}+(\epsilon_1+\epsilon_2)\Big(\frac{\partial^2 N_{\mathrm{T}}}{\partial x^2}-\frac{\partial^2 T(x)}{\partial x^2}+k_{\mathrm{w}}\Big)-\epsilon_1\epsilon_2\Big(\frac{\partial^4 N_{\mathrm{T}}}{\partial x^4}-\frac{\partial^4 T(x)}{\partial x^4}\Big)\Big)\frac{\partial^2 w}{\partial x^2}\\
&+\Big(\frac{\partial T(x)}{\partial x}-\frac{\partial N_{\mathrm{T}}}{\partial x}+(\epsilon_1+\epsilon_2)\Big(\frac{\partial^3 N_{\mathrm{T}}}{\partial x^3}-\frac{\partial^3 T(x)}{\partial x^3}\Big)\Big)\frac{\partial w}{\partial x}-k_{\mathrm{w}}w\\
&-k_{\mathrm{d}}\Big(\frac{\partial w}{\partial t}-(\epsilon_1+\epsilon_2)\frac{\partial^3 w}{\partial x^2\partial t}+\epsilon_1\epsilon_2\frac{\partial^5 w}{\partial x^4\partial t}\Big)\\
=&-m_0\Big(\frac{\partial^2 w}{\partial t^2}-(\epsilon_1+\epsilon_2)\frac{\partial^4 w}{\partial x^2\partial t^2}+\epsilon_1\epsilon_2\frac{\partial^6 w}{\partial x^4\partial t^2}\Big),
\end{aligned}
\tag{21c}
$$

where

$$\Delta_u=(A_0+2B_0)\frac{\partial^2 u}{\partial x^2}-(\epsilon_2A_0+2\epsilon_1B_0)\frac{\partial^4 u}{\partial x^4}-(A_1+2B_1)\frac{\partial^2\varphi}{\partial x^2}+(\epsilon_2A_1+2\epsilon_1B_1)\frac{\partial^4\varphi}{\partial x^4}, \tag{22a}$$

$$
\begin{aligned}
\Delta_\varphi=&(A_1+2B_1)\frac{\partial^2 u}{\partial x^2}-(\epsilon_2A_1+2\epsilon_1B_1)\frac{\partial^4 u}{\partial x^4}+B_0\varphi-(A_2+2B_2+\epsilon_1B_0)\frac{\partial^2\varphi}{\partial x^2}\\
&+(\epsilon_2A_2+2\epsilon_1B_2)\frac{\partial^4\varphi}{\partial x^4}-B_0\frac{\partial w}{\partial x}+\epsilon_1B_0\frac{\partial^3 w}{\partial x^3},
\end{aligned}
\tag{22b}
$$

$$\Delta_w=B_0\frac{\partial\varphi}{\partial x}-\epsilon_1B_0\frac{\partial^3\varphi}{\partial x^3}+\epsilon_1B_0\frac{\partial^4 w}{\partial x^4}-B_0\frac{\partial^2 w}{\partial x^2}. \tag{22c}$$

Because the current study is about wave dispersion in unbounded elastic domains, there is no need to discuss and consider the boundary conditions[49–51].

5 Solution procedure

In this section, to describe wave dispersion in Kelvin-Voigt rotating nanobeams, the analytical solution is provided to the governing equations. The displacement fields associated with wave propagation can be illustrated using the harmonic method as follows[36,39]:

$$\begin{cases} u(x,t)=u_0\exp(\mathrm{i}(Kx-\omega t)),\\ \varphi(x,t)=\varphi_0\exp(\mathrm{i}(Kx-\omega t)),\\ w(x,t)=w_0\exp(\mathrm{i}(Kx-\omega t)), \end{cases} \tag{23}$$

in which ω and K are the frequency and wave number, respectively, $\boldsymbol{X}\,(=(u_0,\varphi_0,w_0))$ is the wave amplitude matrix, and $\mathrm{i}=\sqrt{-1}$.

By substituting Eq. (23) and its derivatives into Eq. (21), the characteristic equation is obtained as

$$(\boldsymbol{K}+\omega\boldsymbol{C}+\omega^2\boldsymbol{M})\boldsymbol{X}=\boldsymbol{0}, \tag{24}$$

where $\boldsymbol{M},\boldsymbol{C}$, and $\boldsymbol{K}$ are the mass, damping, and stiffness matrices, respectively, and

$$\boldsymbol{M}=\begin{bmatrix} m_{u_0u_0} & m_{u_0\varphi_0} & m_{u_0w_0}\\ m_{\varphi_0u_0} & m_{\varphi_0\varphi_0} & m_{\varphi_0w_0}\\ m_{w_0u_0} & m_{w_0\varphi_0} & m_{w_0w_0}\end{bmatrix},\quad \boldsymbol{K}=\begin{bmatrix} k_{u_0u_0} & k_{u_0\varphi_0} & k_{u_0w_0}\\ k_{\varphi_0u_0} & k_{\varphi_0\varphi_0} & k_{\varphi_0w_0}\\ k_{w_0u_0} & k_{w_0\varphi_0} & k_{w_0w_0}\end{bmatrix},\quad \boldsymbol{C}=\begin{bmatrix} c_{u_0u_0} & c_{u_0\varphi_0} & c_{u_0w_0}\\ c_{\varphi_0u_0} & c_{\varphi_0\varphi_0} & c_{\varphi_0w_0}\\ c_{w_0u_0} & c_{w_0\varphi_0} & c_{w_0w_0}\end{bmatrix}. \tag{25}$$

As a standard description, the eigenvalue problem in Eq. (24) can be stated as follows:

$$\begin{bmatrix} -\boldsymbol{M}^{-1}\boldsymbol{C} & -\boldsymbol{M}^{-1}\boldsymbol{C}\\ \boldsymbol{I} & \boldsymbol{0}\end{bmatrix}\begin{bmatrix}\dot{\boldsymbol{X}}\\ \boldsymbol{X}\end{bmatrix}=\omega\begin{bmatrix}\dot{\boldsymbol{X}}\\ \boldsymbol{X}\end{bmatrix}. \tag{26}$$

Equation (26) is an eigenvalue problem, and TA, LA, and torsional (TO) wave frequencies can be easily estimated by setting the determinant of the above matrix to zero. Also, the phase velocity of waves ($V_{\mathrm{c}}=\omega/K$), escape frequency ($K\to\infty$), and cut-off frequency ($K\to 0$) can be easily computed.

6 Results and discussion

6.1 Model validation

This section shows numerical results concerning the propagation frequencies and phase velocities of various elastic wave types in the rotating viscoelastic nanobeam. To validate the findings presented in this paper, the propagation frequencies of LA and TA waves in BaO materials are determined using the model and solution method described herein. Figure 2 provides a comparison between the results presented in Ref. [47] and the results obtained in this study, confirming the accuracy of the model and method employed.

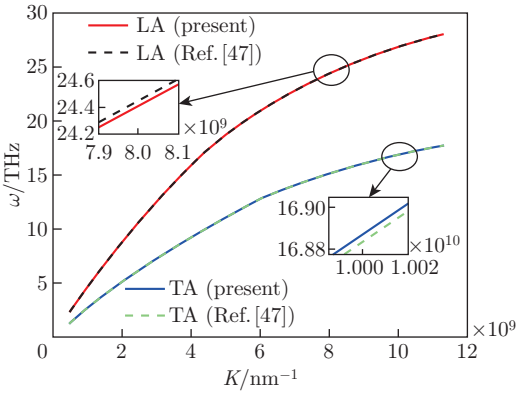

Fig. 2 Model validation (color online)

Following the validation process, the mechanical and physical properties of gold (Au), as provided in Refs. [38] and [47], are utilized to extract the results. Table 1 presents these properties along with the geometric characteristics of the rotating nanobeam.

Table 1 Mechanical and geometric characteristics of rotating nanobeam

λ/GPa	μ/GPa	$\rho/(\mathrm{kg}\cdot\mathrm{m}^{-3})$	a/nm	$\alpha/^{\circ}\mathrm{C}^{-1}$
154	48	10 490	0.407 9	14.2×10^{-6}
ϵ_1/nm^2	ϵ_2/nm^2	h/nm	b/nm	L/nm
$0.14a^2$	$0.018a^2$	1	2	15

The obtained results focus on the propagation frequencies and phase velocities of elastic waves, taking into account various factors, namely nonlocal parameters, Kelvin-Voigt coefficient, nanobeam rotating speed, temperature gradient, Winkler and Pasternak coefficients, and foundation damping. These factors are comprehensively examined and discussed. To ensure accurate results, the wave number varies from zero to its maximum value $\left(K_{\max}=\frac{2\pi}{a}\right)$.

6.2 Effects of nonlocal parameters

In the general nonlocal elasticity method, the behaviour of the nanostructure is described using two distinct nonlocal coefficients, namely ϵ_1 and ϵ_2. Therefore, Fig. 3 illustrates the impacts of changes in these coefficients on the propagation frequencies and phase velocities of LA, TO, and TA waves. To obtain the results, the value of ϵ_1 is kept fixed, while the ratio ϵ_1/ϵ_2 is varied in five steps from 0.1 to 2 for phase velocity results, and in eight steps from 0.1 to 10 for propagation frequency results. This stepwise variation allows for a comprehensive analysis of the influence of these coefficients on the wave behaviour.

The results of propagation frequency for LA, TO, and TA waves are shown in Figs. 3(a), 3(c), and 3(e), respectively. According to the results, it is clear that, with the increase in the ratio

ϵ_1/ϵ_2, which means a decrease in the value of ϵ_2, the corresponding propagation frequencies of all three types of waves increase due to the increase in the stiffness of the rotating nanobeam.

In fact, the increase in ϵ_1/ϵ_2 due to the decrease in ϵ_2, causes the nanobeam to become stiffener, and consequently increases the frequencies of all three types of waves in the nanobeam. Also, Figs. 3(b), 3(d), and 3(f) display the results of phase velocities for LA, TO, and TA waves, respectively. With the increase in the wave number k, the phase velocities for all types of waves decrease. However, the increase in ϵ_1/ϵ_2 due to the increase in the propagation frequency causes the increment of phase velocities of all three types of waves. As concluded previously in Sections 1–3, the results presented for $\epsilon_1 = \epsilon_2$ in Fig. 3 are the same results obtained from the ENT.

According to the results of Fig. 3, it can be concluded that, for materials such as copper (Cu), gold (Au), platinum (Pt), and silicon (Si), with two different nonlocal coefficients ϵ_1 and ϵ_2, the application of Eringen's nonlocal elasticity for describing the elastic wave behaviour in the structure will lead to a significant error.

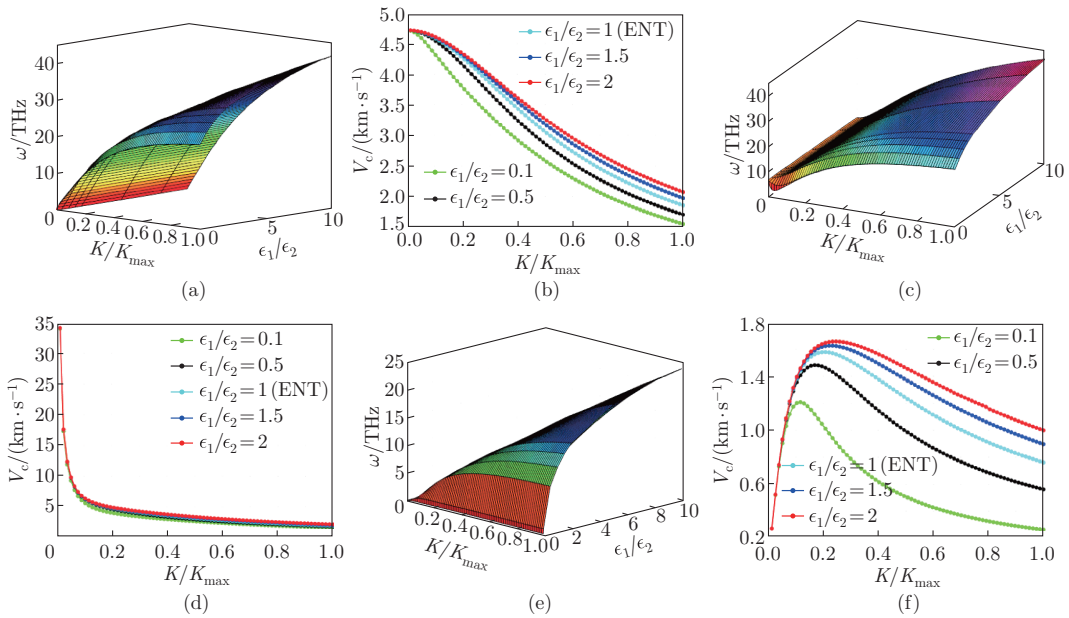

Fig. 3 Effects of nonlocal parameters on (a) LA wave frequency, (b) LA phase velocity, (c) TO wave frequency, (d) TO phase velocity, (e) TA wave frequency, and (f) TA phase velocity (color online)

6.3 Effects of Kelvin-Voigt coefficient

Figure 4 shows the effects of changes in Kelvin-Voigt structural damping coefficient (C_{d}) on the propagation frequencies and phase velocities of all three types of LA, TO, and TA waves. With the increase in the Kelvin-Voigt coefficient, the propagation frequencies of all three types of waves in the viscoelastic nanobeam decrease and reach zero with the increase in the wave number. In other words, it can be concluded that, by increasing the Kelvin-Voigt coefficient, and for values greater than a certain value of $K/K_{\max}$, the propagation of all three types of waves in the viscoelastic nanobeam is stopped, and no wave will be able to propagate in the viscoelastic nanobeam. Since the necessary condition for wave propagation in a medium is the existence of elastic properties in that medium, with the increase in C_{d} and for wave numbers greater than a certain value (for example, in the LA wave in Au element for $C_{\mathrm{d}} = 0.1$ ps and $K/K_{\max} \geqslant 0.376$), the wave propagation, i.e., the energy transfer within the structure, stops

due to hysteretic losses. In fact, the increase in C_{d} means that the viscoelastic nanobeam shows the change of its elastic properties in the form of energy loss, which is the main reason for the lack of wave propagation in the viscoelastic nanobeam and for certain values of the wave number.

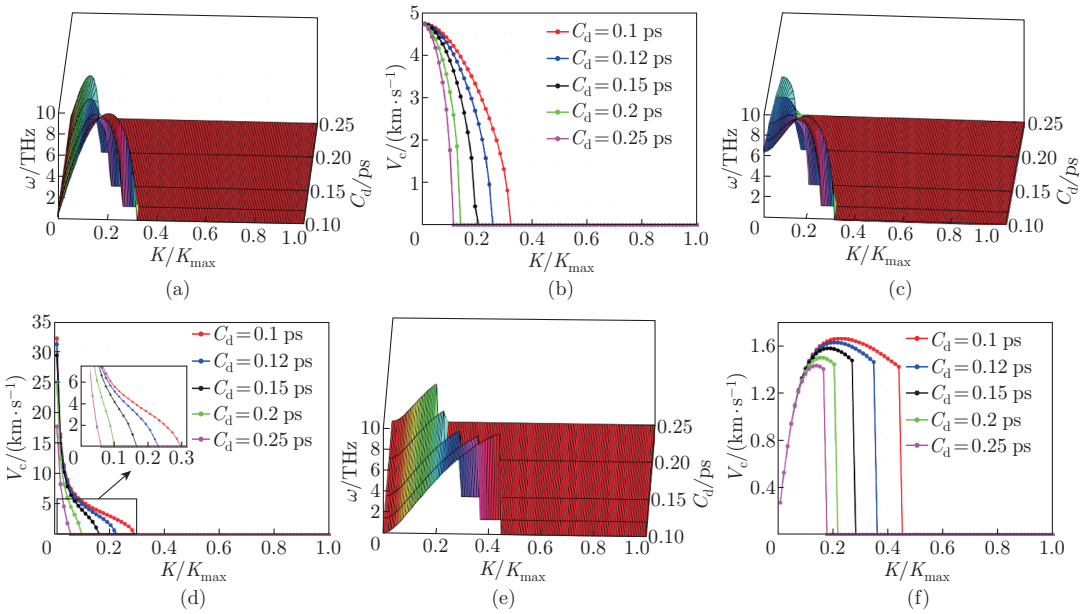

Fig. 4 Effects of Kelvin-Voigt viscoelastic coefficient on (a) LA wave frequency, (b) LA phase velocity, (c) TO wave frequency, (d) TO phase velocity, (e) TA wave frequency, and (f) TA phase velocity (color online)

The results are similar for phase velocities. In other words, with the increase in C_{d}, both propagation frequencies and phase velocities decrease. Also, for larger values of C_{d}, the wave propagation is stopped for smaller values of $K/K_{\max}$, and consequently the phase velocity becomes zero. The important point is that, for the same value of C_{d}, the stopping of the wave propagation in the Kelvin-Voigt viscoelastic nanobeam will occur for the TO wave at smaller values of $K/K_{\max}$ than the other two types of waves. Also, the TA wave stops for higher values of $K/K_{\max}$. In other words, the increase in C_{d} has more effects on the stopping of the TO wave than the TA wave.

6.4 Effects of nanobeam rotating speed

Figure 5 shows the effects of the rotating speed of the nanobeam on the propagation frequencies of TO and TA waves in a specific value of the wave number ($K = 10\,\mathrm{nm}^{-1}$). According to Eq. (7), the value of $T(x)$ is a function of the position x in the length of the beam. Therefore, when deriving the results, the position of the wave in the length of the beam should also be taken into account. Hence, to extract the results of TA and TO wave propagation frequencies, the value of x and the rotating speed of the nanobeam change from 0 nm to 15 nm and 0 THz to 0.3 THz, respectively. Based on the results, it is obvious that, the propagation frequencies of TO and TA waves increase with the increase in the rotational speed of the nanobeam. Because the increment of the rotating speed increases the value of the centrifugal force which always acts as a tensile force on the nanobeam, and consequently the equivalent hardness of the rotating nanobeam increases. Importantly, the effect of the rotating speed of the nanobeam on the TO and TA frequencies gradually disappears when TO and TA waves approach the end of the rotating nanobeam (at $x = 15\,\mathrm{nm}$). Because at the beginning of the nanobeam, the acting

tensile force on the nanobeam has a maximum value, and with the increment of the length of the beam, this value decreases, and finally at the end of the nanobeam, this tensile force vanishes. In fact, due to the rotation of the nanobeam, the equivalent hardness is maximum at the beginning of the nanobeam and is minimum at the end.

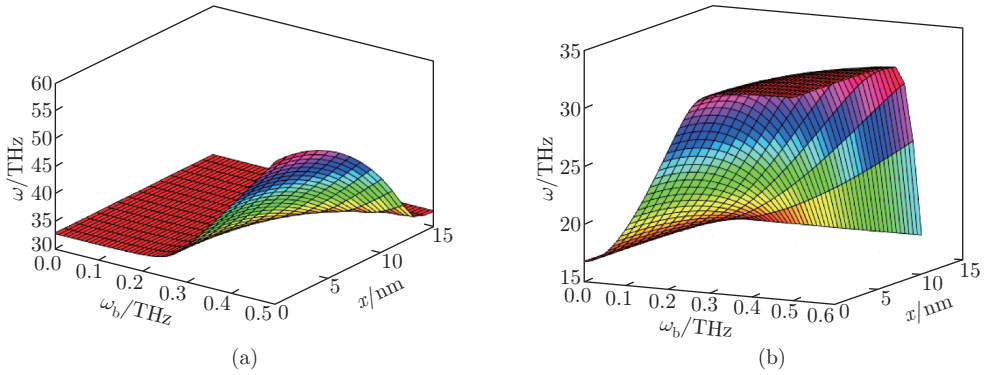

Fig. 5 Effects of rotating speed of nanobeam on frequency at $K = 10\,\mathrm{nm}^{-1}$ for (a) TO wave and (b) TA wave (color online)

From Fig. 5(a), which shows the effects of the rotating speed of the rotating nanobeam on the frequency for the TO wave, it is clear that the slope of frequency increment at low rotational speeds is very gentle, but it becomes steep as the rotational speed of the nanobeam increases. Also, it can be concluded that the slope of increasing frequency for larger wave numbers is steeper than that for lower wave numbers.

According to Fig. 5(b), it can be concluded that, increasing the rotating speed of the nanobeam up to a certain value, increases the frequency of the TA wave, and for values greater than that certain value, it will no longer have an effect on the frequency of the TA wave. In other words, by increasing the rotational speed of the nanobeam, the frequency of the TA wave will converge to its final value, which strongly depends on the wave number.

Figure 6 illustrates the gradient of phase velocity based on the variation of $K/K_{\max}$ at five different positions of the beam for the TO wave. The results in Fig. 6 are presented for two cases $C_\mathrm{d} = 0\,\mathrm{ps}$, $\omega_\mathrm{b} = 0.3\,\mathrm{THz}$ (see Fig. 6(a)) and $C_\mathrm{d} = 0.1\,\mathrm{ps}$, $\omega_\mathrm{b} = 0.3\,\mathrm{THz}$ (see Fig. 6(b)). The results show that the position of the TO wave along the nanobeam has no significant effects on the phase velocity of the TO wave. Also, the effect of C_d which is extensively discussed in

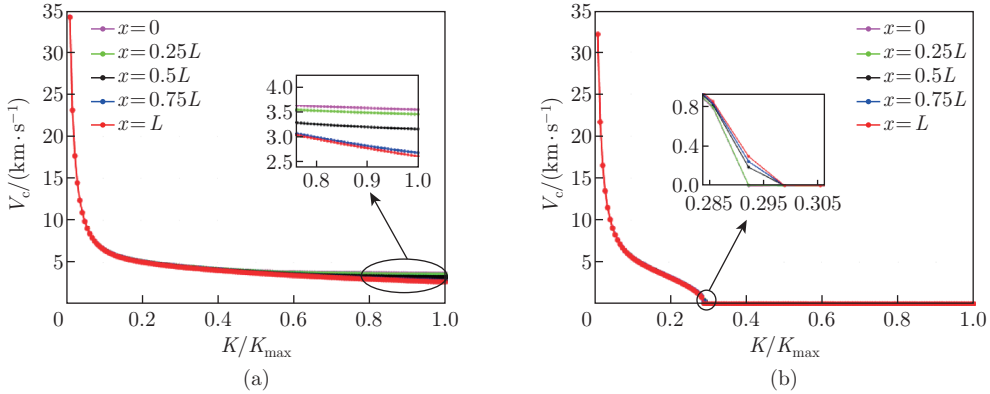

Fig. 6 Variations of phase velocity at different positions of beam for TO wave, (a) $C_\mathrm{d} = 0\,\mathrm{ps}$, $\omega_2 = 0.3\,\mathrm{THz}$ and (b) $C_\mathrm{d} = 0.1$ ps, $\omega_\mathrm{b} = 0.3\,\mathrm{THz}$ (color online)

Subsection 6.3 can be easily noticed in Fig. 6(b).

Figures 7 and 8 display the variations of phase velocity for the TA wave under different conditions. The results are presented to observe and investigate the effects of the rotational speed of the nanobeam, the position of the wave along the nanobeam, and the Kelvin-Voigt coefficient on the phase velocity for the TA wave.

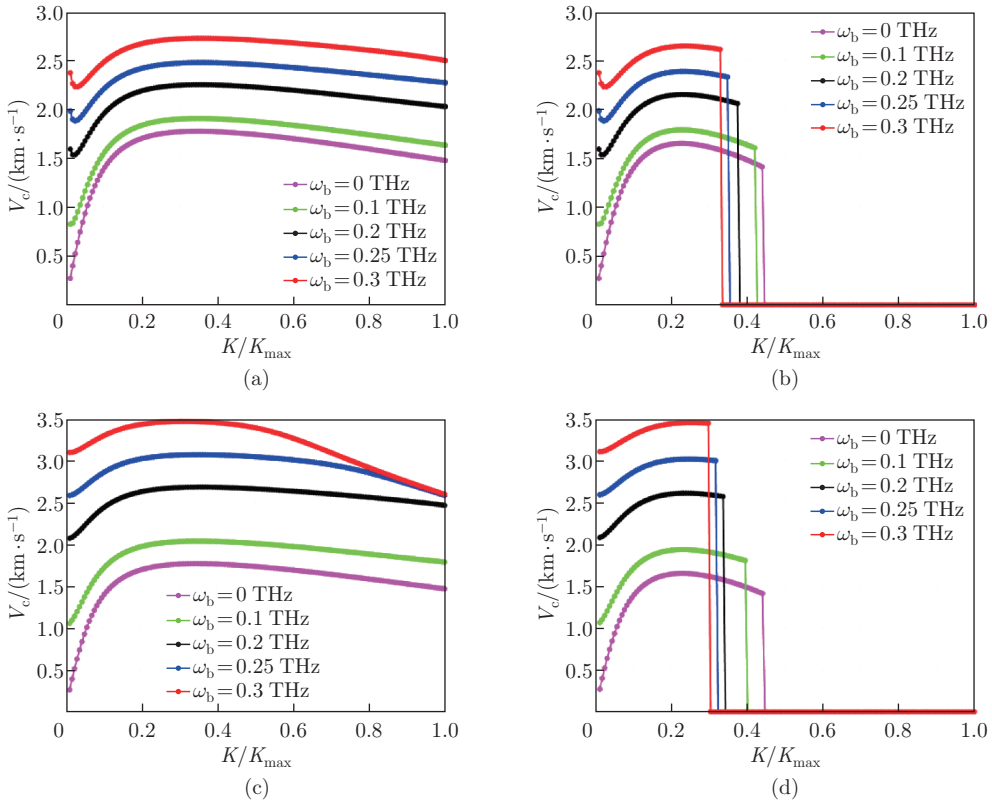

Fig. 7 Effects of rotating speed of nanobeam on phase velocity for TA wave, (a) $C_{\mathrm{d}} = 0\,\mathrm{ps}$, $x = 0.75L$, (b) $C_{\mathrm{d}} = 0.1\,\mathrm{ps}$, $x = 0.75L$, (c) $C_{\mathrm{d}} = 0\,\mathrm{ps}$, $x = 0.25L$, and (d) $C_{\mathrm{d}} = 0.1\,\mathrm{ps}$, $x = 0.25L$ (color online)

As found in Fig. 7, with the increase in the rotational speed of nanobeam, the phase velocity for the TA wave increases. In addition, the amount and the process of the increment depend on both values of $K/K_{\max}$ and the position of the TA wave. Also, when $C_{\mathrm{d}} \neq 0\,\mathrm{ps}$, with the increase in the rotational speed of the nanobeam, the TA wave stops for lower values of $K/K_{\max}$. However, for the rotating nanobeam, stopping the TA wave also depends on the position of the TA wave along the nanobeam.

For example, based on the results in Figs. 7(b) and 7(d), in the case $C_{\mathrm{d}} = 0.1\,\mathrm{ps}$, $\omega_{\mathrm{b}} = 0.3\,\mathrm{THz}$, the TA wave stops at $x = 0.25L$ when $K/K_{\max} \geqslant 0.304$ and stops at $x = 0.75L$ when $K/K_{\max} \geqslant 0.336$. The same results can also be concluded by comparing Figs. 8(b) and 8(d). Moreover, Figs. 8(a) and 8(c) show the effect of the TA wave position along the beam on the phase velocity. The value of phase velocity at the beginning of the rotating nanobeam is maximum, especially for lower values of $K/K_{\max}$ and ω_{b}.

6.5 Effects of temperature gradient

The effects of temperature gradient on the propagation frequencies of LA, TO, and TA waves for the rotating nanobeam are shown in Fig. 9. To extract the results, the reference temperature

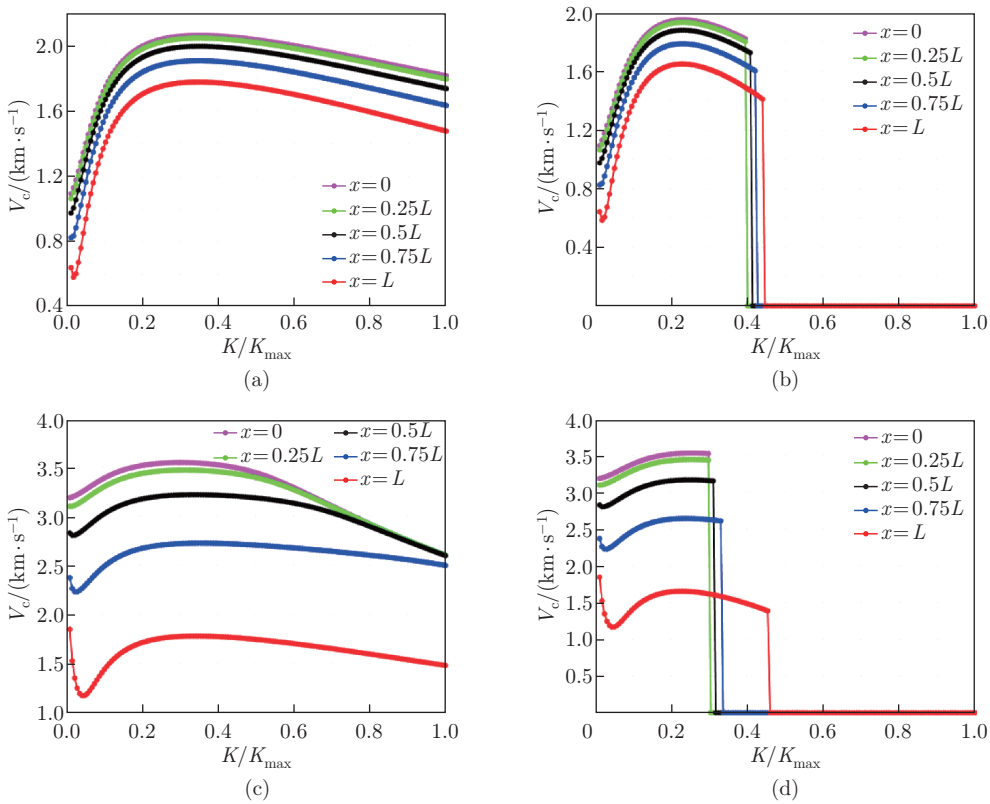

Fig. 8 Variations of phase velocity at different positions of beam for TA wave, (a) $C_\mathrm{d} = 0\,\mathrm{ps}$, $\omega_\mathrm{b} = 0.1\,\mathrm{THz}$, (b) $C_\mathrm{d} = 0.1\,\mathrm{ps}$, $\omega_\mathrm{b} = 0.1\,\mathrm{THz}$, (c) $C_\mathrm{d} = 0\,\mathrm{ps}$, $\omega_\mathrm{b} = 0.3\,\mathrm{THz}$, and (d) $C_\mathrm{d} = 0.1\,\mathrm{ps}$, $\omega_\mathrm{b} = 0.3\,\mathrm{THz}$ (color online)

is observed as $T_0 = 20\,^\circ\mathrm{C}$, and the temperature gradient is considered along the nanobeam thickness from $\Delta T = 0\,^\circ\mathrm{C}$ to $\Delta T = 35\,^\circ\mathrm{C}$. Based on the obtained results, the temperature gradient has no effects on the frequency of the LA wave, a slight effect on the frequency of the TO wave, while a significant effect on the frequency of the TA wave.

According to Figs. 9(a) and 9(c), TA and TO wave frequencies decrease with the temperature gradient. Also, the increase in the temperature causes the delay of initiating the TA wave propagation and reduces the range of TA wave propagation in terms of the wave number in the rotating nanobeam. Therefore, with the increase in temperature, the TA wave propagates for larger wave numbers, and with a further increase in the wave number, the frequency approaches zero again, and the TA wave stops propagating in the rotating nanobeam. As shown in Figs. 9(b) and 9(d), the temperature gradient does not significantly affect the phase velocity of TO waves, but has the same effect on the phase velocity of TA waves as the effect on the propagation frequency.

6.6 Effects of Winkler coefficient

The effects of Winkler coefficient of foundation on the frequencies and phase velocities of TO and TA waves are considered in Fig. 10. On the basis of the results, the increase in the Winkler coefficient due to the increase in the stiffness of the nanobeam, increases the frequencies of both TO and TA waves. As is obvious in Fig. 10(a), with the increase in the wave number, the effect of Winkler coefficient on the frequency of TO wave decreases and disappears for larger values of the wave number.

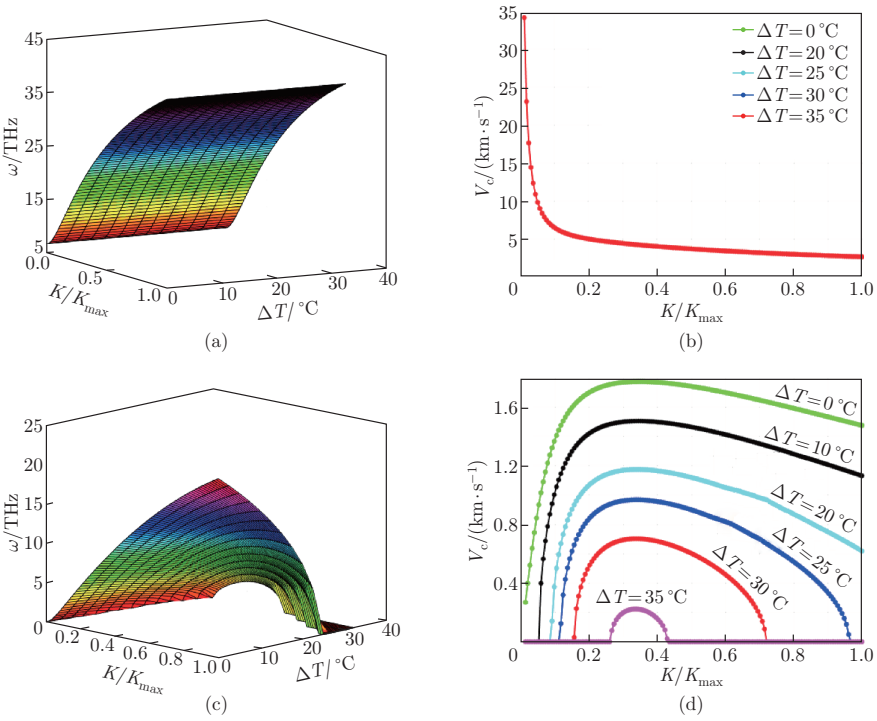

Fig. 9 Effects of temperature gradient on (a) TO wave frequency, (b) TO phase velocity, (c) TA wave frequency, and (d) TA phase velocity (color online)

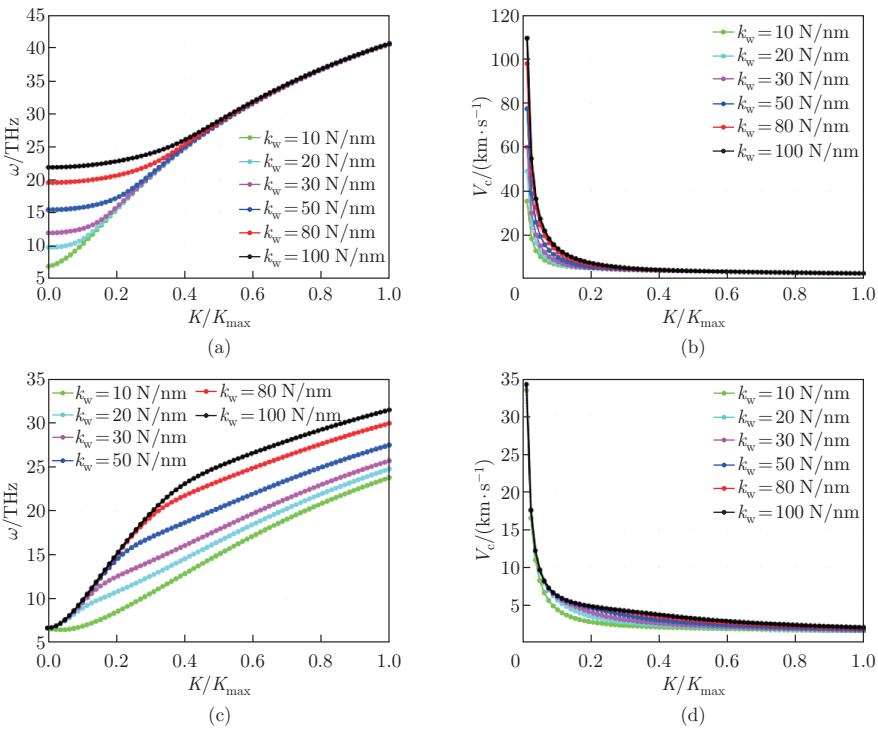

Fig. 10 Effects of Winkler coefficient on (a) TO wave frequency, (b) TO phase velocity, (c) TA wave frequency, and (d) TA phase velocity (color online)

6.7 Effects of Pasternak coefficient

Figure 11 illustrates the effects of Pasternak coefficient of foundation on the frequencies and phase velocities of TO and TA waves. According to Figs. 11(a) and 11(c) and due to the increase in the stiffness of the nanobeam, TO and TA frequencies increase with the increase in the Pasternak coefficient. However, for $k_p \geqslant 0.4$, the effect of Pasternak coefficient of foundation on the TA wave frequency is negligible.

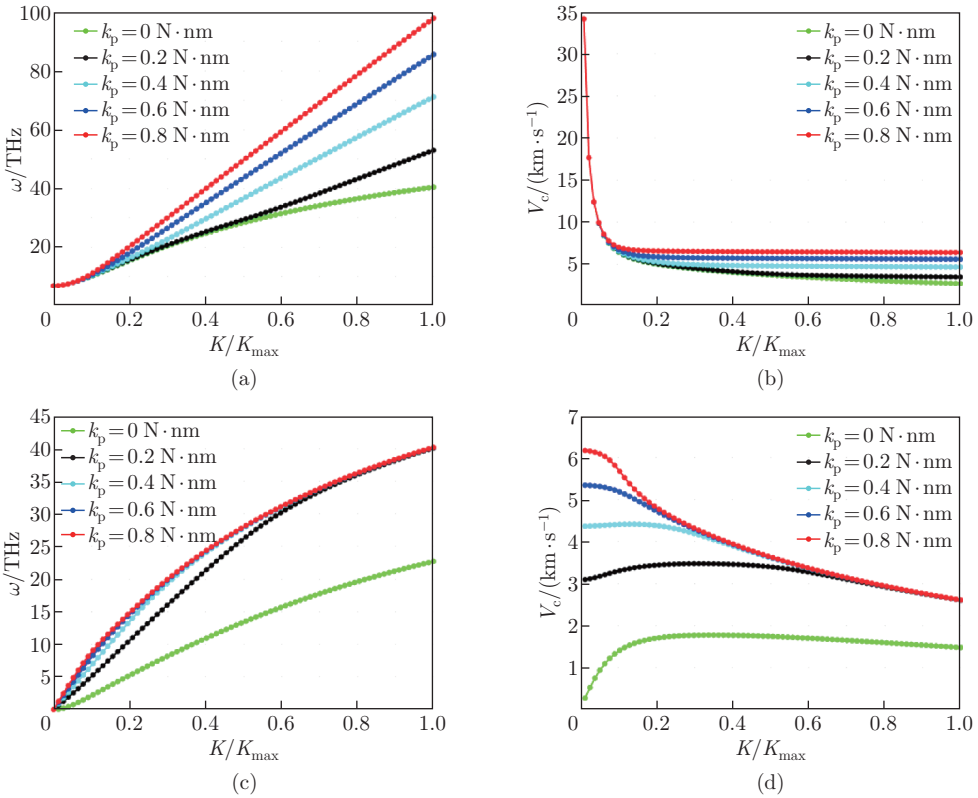

Fig. 11 Effects of Pasternak coefficient on (a) TO wave frequency, (b) TO phase velocity, (c) TA wave frequency, and (d) TA phase velocity (color online)

The study on the effects of Pasternak coefficient on the phase velocity can also be found in Figs. 11(b) and 11(d). It is shown that the effect of Pasternak coefficient on the phase velocity of the TO wave increases with an increase in K/K_{max}, whereas it is vice versa for the TA wave and vanishes with an increase in K/K_{max}.

6.8 Effects of foundation damping

Based on Fig. 12, with the increase in the viscoelastic damping coefficient of foundation, the propagations of TO and TA waves are delayed up to a certain value of K/K_{max}. It means that, for a smaller value of K/K_{max}, the TO and TA waves cannot propagate in the nanobeam, but with the increase in the value of K/K_{max}, the TA wave gradually and the TO wave instantly start to propagate. In fact, the viscoelastic damping property of the foundation acts as a resistance factor against wave propagation, and the wave energy for smaller values of K/K_{max} has the ability to overcome the viscoelastic damping energy of the foundation.

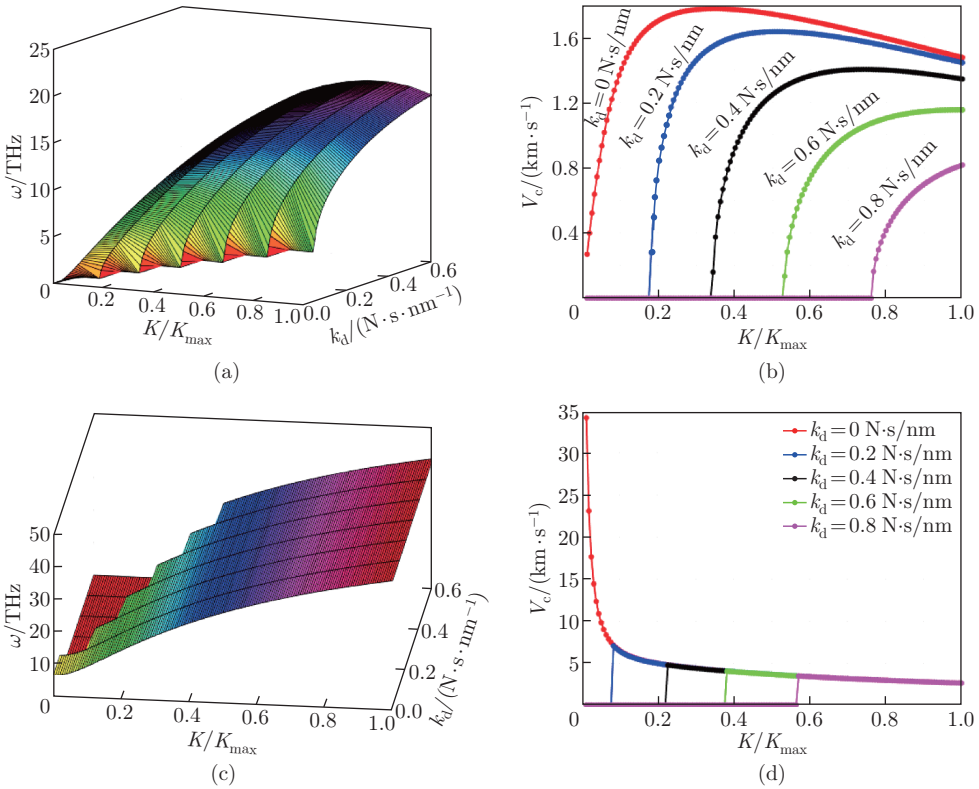

Fig. 12 Effects of foundation damping coefficient on (a) TA wave frequency, (b) TA phase velocity, (c) TO wave frequency, and (d) TO phase velocity (color online)

7 Conclusions

This research encompasses a comprehensive investigation into the propagation characteristics of LA, TO, and TA waves for a rotating Kelvin-Voigt viscoelastic nanobeam supported on a viscoelastic foundation. The governing equations of motion and mathematical model for the rotating viscoelastic nanobeam are derived using the GNT in conjunction with the Timoshenko beam model. Analytical methods are used to extract the results, and the effects of various factors such as nonlocal parameters, Kelvin-Voigt coefficient, viscoelastic foundation coefficients, and nanobeam rotation speed on wave propagation behaviors are thoroughly examined. The significant findings obtained in this research can be summarized as follows.

(i) The ENT, which is a simplified form of the GNT, does not accurately predict the mechanical and wave propagation behaviors in materials with $\epsilon_1 \neq \epsilon_2$, such as gold and copper. Therefore, it is recommended to utilize the GNT instead of the ENT to achieve more accurate analyses of wave propagation phenomena.

(ii) Increasing the ratio ϵ_1/ϵ_2 leads to a larger frequency of propagation for all three types of LA, TO, and TA waves due to the increasing stiffness of the nanobeam.

(iii) As the Kelvin-Voigt viscoelastic coefficient C_d increases, the propagation frequencies of all three types of waves decrease. Moreover, as the wave number increases, the propagation frequency approaches zero, indicating a cessation of wave propagation and energy transfer within the structure due to hysteretic losses. It is worth noting that the effect of C_d is more pronounced on the attenuation of the TO wave than the TA wave.

(iv) The rotational speed of the nanobeam influences the equivalent stiffness of the rotating

structure through the centrifugal force. Consequently, the propagation frequencies of TO and TA waves increase with an increase in the rotational speed of the nanobeam.

(v) The temperature gradient significantly affects the frequency of the TA wave, while it has a relatively minor impact on the frequency of the TO wave.

Conflict of interest The authors declare no conflict of interest.

References

[1] ATTIA, M. A. Investigation of size-dependent quasistatic response of electrically actuated nonlinear viscoelastic microcantilevers and microbridges. *Meccanica*, **52**, 2391–2420 (2017)

[2] ELTAHER, M. A., SHANAB, R. A., and MOHAMED, N. A. Analytical solution of free vibration of viscoelastic perforated nanobeam. *Archive of Applied Mechanics*, **93**(1), 221–243 (2023)

[3] RAHMANIAN, S. and HOSSEINI-HASHEMI, S. Size-dependent resonant response of a double-layered viscoelastic nanoresonator under electrostatic and piezoelectric actuations incorporating surface effects and Casimir regime. *International Journal of Non-Linear Mechanics*, **109**, 118–131 (2019)

[4] CABAN, S., AYTEKIN, E., SAHIN, A., and CAPAN, Y. Nanosystems for drug delivery. *Drug Design and Delivery*, **2**(1), 2 (2014)

[5] CAO, D. Y. and WANG, Y. Q. Wave dispersion in viscoelastic lipid nanotubes conveying viscous protein solution. *The European Physical Journal Plus*, **135**, 24 (2020)

[6] SARPARAST, H., ALIBEIGLOO, A., BORJALILOU, V., and KOOCHAKIANFARD, O. Forced and free vibrational analysis of viscoelastic nanotubes conveying fluid subjected to moving load in hygro-thermo-magnetic environments with surface effects. *Archives of Civil and Mechanical Engineering*, **22**(4), 172 (2022)

[7] MARTINS-JÚNIOR, P. A., ALCÂNTARA, C. E., RESENDE, R. R., and FERREIRA, A. J. Carbon nanotubes: directions and perspectives in oral regenerative medicine. *Journal of Dental Research*, **92**(7), 575–583 (2013)

[8] ANSARI, R., NESARHOSSEINI, S., FARAJI-OSKOUIE, M., and ROUHI, H. Size-dependent buckling analysis of piezoelectric nanobeams resting on elastic foundation considering flexoelectricity effect using the stress-driven nonlocal model. *The European Physical Journal Plus*, **136**, 876 (2021)

[9] ZAREPOUR, M., HOSSEINI, S. A., and GHADIRI, M. Free vibration investigation of nano mass sensor using differential transformation method. *Applied Physics A*, **123**, 1–10 (2017)

[10] ALSHENAWY, R., SAHMANI, S., SAFAEI, B., ELMOGHAZY, Y., AL-ALWAN, A., and AL NUWAIRAN, M. Surface stress effect on nonlinear dynamical performance of nanobeam-type piezoelectric energy harvesters via meshless collocation technique. *Engineering Analysis with Boundary Elements*, **152**, 104–119 (2023)

[11] ALI, F., RAZA, W., LI, X., GUL, H., and KIM, K. H. Piezoelectric energy harvesters for biomedical applications. *Nano Energy*, **57**, 879–902 (2019)

[12] WANG, Y., HONG, M., VENEZUELA, J., LIU, T., and DARGUSCH, M. Expedient secondary functions of flexible piezoelectrics for biomedical energy harvesting. *Bioactive Materials*, **22**, 291–311 (2023)

[13] EBRAHIMI, F. and BARATI, M. R. Damping vibration behavior of viscoelastic porous nanocrystalline nanobeams incorporating nonlocal-couple stress and surface energy effects. *Iranian Journal of Science and Technology, Transactions of Mechanical Engineering*, **43**, 187–203 (2019)

[14] NADERI, A., BEHDAD, S., and FAKHER, M. Size dependent effects of two-phase viscoelastic medium on damping vibrations of smart nanobeams: an efficient implementation of GDQM. *Smart Materials and Structures*, **31**(4), 045007 (2022)

[15] EL-MOUMEN, A., TARFAOUI, M., NACHTANE, M., and LAFDI, K. Carbon nanotubes as a player to improve mechanical shock wave absorption. *Composites Part B: Engineering*, **164**, 67–71 (2019)

[16] WANG, X., WU, S., YIN, J., MORADI, Z., SAFA, M., and KHADIMALLAH, M. A. On the electromechanical energy absorption of the reinforced composites piezoelectric MEMS via adaptive neuro-fuzzy inference system and MCS theory. *Composite Structures*, **303**, 116246 (2023)

[17] LIU, H., LIU, H., and YANG, J. Vibration of FG magneto-electro-viscoelastic porous nanobeams on visco-Pasternak foundation. *Composites Part B*: *Engineering*, **155**, 244–256 (2018)

[18] BAGHERI, R. and TADI-BENI, Y. On the size-dependent nonlinear dynamics of viscoelastic/flexoelectric nanobeams. *Journal of Vibration and Control*, **27**(17-18), 2018–2033 (2021)

[19] ERINGEN, A. C. Nonlocal continuum mechanics based on distributions. *International Journal of Engineering Science*, **44**(3-4), 141–147 (2006)

[20] LI, C., ZHU, C., LIM, C. W., and LI, S. Nonlinear in-plane thermal buckling of rotationally restrained functionally graded carbon nanotube reinforced composite shallow arches under uniform radial loading. *Applied Mathematics and Mechanics* (*English Edition*), **43**(12), 1821–1840 (2022) https://doi.org/10.1007/s10483-022-2917-7

[21] LAM, D. C., YANG, F., CHONG, A. C. M., WANG, J., and TONG, P. Experiments and theory in strain gradient elasticity. *Journal of the Mechanics and Physics of Solids*, **51**(8), 1477–1508 (2003)

[22] DINDARLOO, M. H. and LI, L. Vibration analysis of carbon nanotubes reinforced isotropic doubly-curved nanoshells using nonlocal elasticity theory based on a new higher order shear deformation theory. *Composites Part B*: *Engineering*, **175**, 107170 (2019)

[23] LAL, R. and DANGI, C. Thermomechanical vibration of bi-directional functionally graded nonuniform Timoshenko nanobeam using nonlocal elasticity theory. *Composites Part B*: *Engineering*, **172**, 724–742 (2019)

[24] SOLTANI, M., ATOUFI, F., MOHRI, F., DIMITRI, R., and TORNABENE, F. Nonlocal elasticity theory for lateral stability analysis of tapered thin-walled nanobeams with axially varying materials. *Thin-Walled Structures*, **159**, 107268 (2021)

[25] TORABI, J., NIIRANEN, J., and ANSARI, R. Nonlinear finite element analysis within strain gradient elasticity: Reissner-Mindlin plate theory versus three-dimensional theory. *European Journal of Mechanics-A/Solids*, **87**, 104221 (2021)

[26] EGHBALI, M., HOSSEINI, S. A., and POURSEIFI, M. Free transverse vibrations analysis of size-dependent cracked piezoelectric nano-beam based on the strain gradient theory under mechanic-electro forces. *Engineering Analysis with Boundary Elements*, **143**, 606–612 (2022)

[27] HU, H., YU, T., and BUI, T. Q. Functionally graded curved Timoshenko microbeams: a numerical study using IGA and modified couple stress theory. *Composite Structures*, **254**, 112841 (2020)

[28] HASSANNEJAD, R., HOSSEINI, S. A., and ALIZADEH-HAMIDI, B. Influence of non-circular cross section shapes on torsional vibration of a micro-rod based on modified couple stress theory. *Acta Astronautica*, **178**, 805–812 (2021)

[29] LIM, C. W., ZHANG, G., and REDDY, J. A higher-order nonlocal elasticity and strain gradient theory and its applications in wave propagation. *Journal of the Mechanics and Physics of Solids*, **78**, 298–313 (2015)

[30] JIN, H., SUI, S., ZHU, C., and LI, C. Axial free vibration of rotating FG piezoelectric nanorods accounting for nonlocal and strain gradient effects. *Journal of Vibration Engineering and Technologies*, **11**(2), 537–549 (2023)

[31] THAI, C. H., FEREIRA, A. J. M., and PHUNG-VAN, P. A nonlocal strain gradient isogeometric model for free vibration analysis of magneto-electro-elastic functionally graded nanoplates. *Composite Structures*, **316**, 117005 (2023)

[32] KHANIKI, H. B. Vibration analysis of rotating nanobeam systems using Eringen's two-phase local/nonlocal model. *Physica E*: *Low-Dimensional Systems and Nanostructures*, **99**, 310–319 (2018)

[33] FANG, J., YIN, B., ZHANG, X., and YANG, B. Size-dependent vibration of functionally graded rotating nanobeams with different boundary conditions based on nonlocal elasticity theory. *Proceedings of the Institution of Mechanical Engineers*, *Part C*: *Journal of Mechanical Engineering Science*, **236**(6), 2756–2774 (2022)

[34] EBRAHIMI, F. and HAGHI, P. Elastic wave dispersion modelling within rotating functionally graded nanobeams in thermal environment. *Advances in Nano Research*, **6**(3), 201 (2018)

[35] EBRAHIMI, F. and DABBAGH, A. Wave dispersion characteristics of rotating heterogeneous magneto-electro-elastic nanobeams based on nonlocal strain gradient elasticity theory. *Journal of Electromagnetic Waves and Applications*, **32**(2), 138–169 (2018)

[36] RAHMANI, A., SAFAEI, B., and QIN, Z. On wave propagation of rotating viscoelastic nanobeams with temperature effects by using modified couple stress-based nonlocal Eringen's theory. *Engineering with Computers*, **38**, 2681–2701 (2022)

[37] EBRAHIMI, F., BARATI, M. R., and HAGHI, P. Wave propagation analysis of size-dependent rotating inhomogeneous nanobeams based on nonlocal elasticity theory. *Journal of Vibration and Control*, **24**(17), 3809–3818 (2018)

[38] SHAAT, M. A general nonlocal theory and its approximations for slowly varying acoustic waves. *International Journal of Mechanical Sciences*, **130**, 52–63 (2017)

[39] FAROUGHI, S., RAHMANI, A., and FRISWELL, M. On wave propagation in two-dimensional functionally graded porous rotating nano-beams using a general nonlocal higher-order beam model. *Applied Mathematical Modelling*, **80**, 169–190 (2020)

[40] RAHMANI, A., FAROUGHI, S., and FRISWELL, M. I. The vibration of two-dimensional imperfect functionally graded (2D-FG) porous rotating nanobeams based on general nonlocal theory. *Mechanical Systems and Signal Processing*, **144**, 106854 (2020)

[41] FAROUGHI, S. and SHAAT, M. Poisson's ratio effects on the mechanics of auxetic nanobeams. *European Journal of Mechanics-A/Solids*, **70**, 8–14 (2018)

[42] LI, H. N., CHENG, L., SHEN, J. P., and YAO, L. Q. Vibration analysis of rotating functionally graded piezoelectric nanobeams based on the nonlocal elasticity theory. *Journal of Vibration Engineering and Technologies*, **9**, 1155–1173 (2021)

[43] WANG, X. Y., LUO, Q. Y., LI, C., and XIE, Z. Y. On the out-of-plane vibration of rotating circular nanoplates. *Transactions of Nanjing University of Aeronautics and Astronautics*, **39**(1), 23–35 (2022)

[44] EBRAHIMI, F. and BARATI, M. R. Effect of three-parameter viscoelastic medium on vibration behavior of temperature-dependent non-homogeneous viscoelastic nanobeams in a hygro-thermal environment. *Mechanics of Advanced Materials and Structures*, **25**(5), 361–374 (2018)

[45] MOHAMMADI, M., SAFARABADI, M., RASTGOO, A., and FARAJPOUR, A. Hygro-mechanical vibration analysis of a rotating viscoelastic nanobeam embedded in a visco-Pasternak elastic medium and in a nonlinear thermal environment. *Acta Mechanica*, **227**, 2207–2232 (2016)

[46] ABOUELREGAL, A. E., AHMAD, H., NOFAL, T. A., and ABU-ZINADAH, H. Thermo-viscoelastic fractional model of rotating nanobeams with variable thermal conductivity due to mechanical and thermal loads. *Modern Physics Letters B*, **35**(18), 2150297 (2021)

[47] SHAAT, M. and ABDELKEFI, A. New insights on the applicability of Eringen's nonlocal theory. *International Journal of Mechanical Sciences*, **121**, 67–75 (2017)

[48] BOYINA, K. and PISKA, R. Wave propagation analysis in viscoelastic Timoshenko nanobeams under surface and magnetic field effects based on nonlocal strain gradient theory. *Applied Mathematics and Computation*, **439**, 127580 (2023)

[49] ZEIGHAMPOUR, H., TADI-BENI, Y., and KARIMIPOUR, I. Material length scale and nonlocal effects on the wave propagation of composite laminated cylindrical micro/nanoshells. *The European Physical Journal Plus*, **132**, 503 (2017)

[50] GOPALAKRISHNAN, S. and NARENDAR, S. *Wave Propagation in Nanostructures*: *Nonlocal Continuum Mechanics Formulations*, Springer Science and Business Media, Germany (2013)

[51] ELTAHER, M. A., KHATER, M. E., and EMAM, S. A. A review on nonlocal elastic models for bending, buckling, vibrations, and wave propagation of nanoscale beams. *Applied Mathematical Modelling*, **40**(5-6), 4109–4128 (2016)